
STRUCTURE AND PROPERTIES
OF THE DEFORMED STATE

Influence of the Deformation Parameters on the Morphology of the Strengthening O Phase and the Mechanical Properties of an Intermetallic VIT5 Titanium Alloy

A. V. Novak^{a, *}, N. A. Nochovnaya^a, and E. B. Alekseev^a

^aAll-Russian Institute of Aviation Materials, Moscow, 105005 Russia

*e-mail: annovak23@gmail.com

Received February 5, 2019; revised February 5, 2019; accepted February 20, 2019

Abstract—The manufacturability of a gadolinium-alloyed intermetallic VIT5 titanium ortho alloy during deformation at temperatures of 800–1100°C is studied. The mechanical properties and the structure of plates rolled according to two deformation regimes are analyzed. The effect of the morphology of the Ti₂AlNb ortho phase on the strength, plastic, and high-temperature properties of the alloy is investigated. The formation of a specified structure is shown to provide a high level of plasticity and high-temperature strength. The relative elongation at 20°C is 7.0%, the tensile strength at 700°C is 950 MPa, and the long-term tensile strength at 700°C for 100 h is 300 MPa.

Keywords: intermetallic VIT5 titanium alloy, ortho alloy, O phase, Ti₂AlNb, deformation, structure, mechanical properties

DOI: 10.1134/S0036029520040205

1. INTRODUCTION

When developing regimern advanced aircraft engines, great attention is paid to the noise and the emission of such harmful substances as CO₂ and NO_x [1, 2] along with improving their energy efficiency and reliability. To solve these problems, new light-weight high-temperature materials with a high level of performance characteristics are developed [3–5]. In particular, high-temperature deformable intermetallic alloys based on the Ti₂AlNb ortho phase (O phase) [7, 8] are considered as effective alternatives for conventional high-temperature titanium pseudo α and ($\alpha + \beta$) alloys, whose operating temperature is limited to 600°C due to high oxidation and severe structure degradation [6].

The successful use of ortho alloys in regimern propulsion engineering requires improved technological and structural ductility without sacrificing a high strength and high heat resistance. Microalloying with rare-earth elements (REEs) is one of the most effective ways to solve this problem. REEs form refractory compounds with oxygen and nitrogen and positively influence the plasticity and structural stability of alloys [9, 10]. Titanium and intermetallic titanium alloys are alloyed with REEs, such as yttrium and gadolinium [10–12]; scandium, cerium, erbium, and dysprosium are used less frequently [13–15]. For example, alloying of a pseudo β VT15 titanium alloy with 0.02 wt % Gd and 0.1 wt % Dy increases the relative

elongation of annealed sheets from 12 to 22%, and alloying with 0.02–0.1 wt % Y almost doubles the plasticity of the alloy. Alloying with yttrium and dysprosium also decreases the oxidation of the VT15 alloy by 1.5–2 times during its heating at 750°C for 1 h [16]. A high-temperature pseudo α VT38 alloy, which contains 0.05–0.2 wt % Gd, surpasses a high-temperature pseudo α VT20 alloy by 40–50% in its mechanical characteristics at temperatures of 500 and 600°C and exhibits the best manufacturability, which allows sheets with a thickness of 0.8 mm instead of 3 mm to be produced [10]. However, the effect of REMs on the structural-phase state and the operating characteristics of ortho alloys is poorly studied [17–20].

This work continues the research of the intermetallic titanium VIT5 ortho alloy created at the All-Russia Institute of Aviation Materials VIAM. We have studied the conditions of ingot melting, the influence of the heat-treatment and rolling parameters on the structure and mechanical properties [21, 22]. This work is aimed at studying the manufacturability of the VIT5 alloy and choosing the optimal deformation regime to form a specified structure and a high level of plasticity and heat resistance.

EXPERIMENTAL

An intermetallic titanium VIT5 ortho alloy with gadolinium microadditives was investigated in the as-cast and deformed states. The composition of the alloy

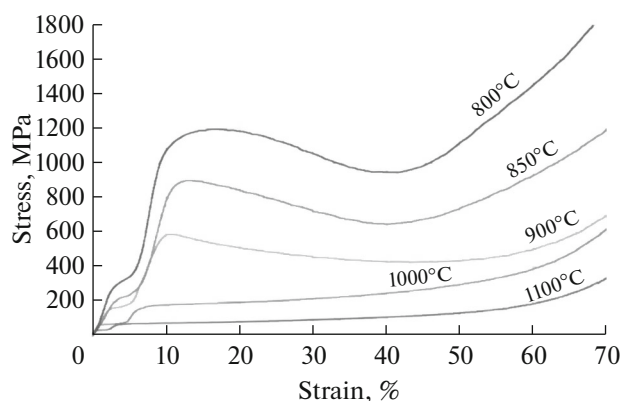


Fig. 1. Stress–strain $\sigma(\epsilon)$ diagrams of the VIT5 alloy tested in the temperature range 800–1100°C.

was as follows (at %): 50.5 Ti, 22.5 Al, 23.5 Nb, and 0.1 Gd. 30-kg VIT5 alloy ingots were produced by three-fold vacuum arc remelting in a ALD Vacuum Technologies VAR L200 system with a consumable electrode. The conditions of the process, which were specified [21, 22], allowed us to exclude the formation of refractory inclusions (niobium) and provided a homogeneous chemical composition throughout the cross-section of the ingot.

Then, plates 20 ± 2 mm thick were prepared from the ingots using the technology including compression, three-dimensional pressing (changing the deformation axis), and hot rolling in the ($\beta/B2 + \alpha_2$) regions. To study the effect of deformation conditions on the structure and the mechanical properties of the alloy, two processing regimes (1, 2) for the production of slabs intended for subsequent rolling were chosen. Deformation regime 2 was characterized by additional forging and an increased holding time at 980°C.

The rolled plates were subjected to two-stage heat treatment in air in a NaberTherm L(N) 15/12 laboratory muffle furnace after deformation. The treatment included heating in the ($\beta/B2 + O + \alpha_2$) region, holding for 2 h, air cooling, subsequent heating in the ($\beta/B2 + O$) region, holding for 12 h, and air cooling.

Cylindrical samples were compressed in the temperature range 800–1100°C to investigate the manufacturability of the cast alloy¹. Samples 10 mm in diameter and 15 mm in gage height were cut longitudinally from an ingot. They had technological grooves at both ends for graphite lubrication used to reduce friction forces. Tests were carried out using an MTS-50 servohydraulic tester at a force of 1600 tf and a deformation rate of 10^{-2} s^{-1} to a deformation of 70%.

¹ The test temperature range was chosen taking into account the conditions of deformation of VT1-4 ortho alloys. The samples were not compressed at higher temperatures, because the alloy has a high technological plasticity and its behavior is similar to that of REE-free ortho alloys at temperatures above $1115 \pm 5^\circ\text{C}$ (in a single-phase $\beta/B2$ region) [23].

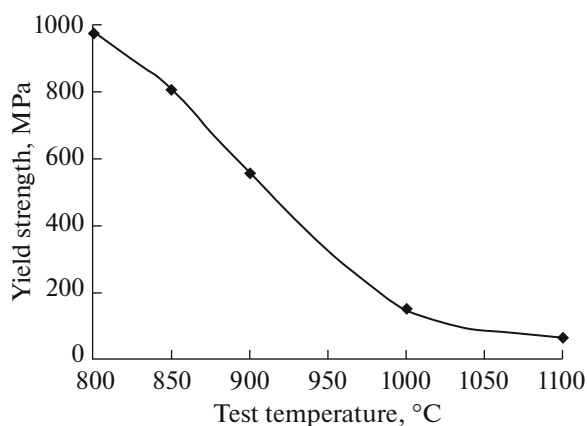


Fig. 2. Yield strength of the VIT5 alloy as a function of temperature.

To determine the mechanical properties, rolled samples were subjected to tensile tests at 20 and 700°C on a Tiratest 2300/1 testing machine according to standard GOST 1497–84 and 9651–84. The long-term (100 h) strength at 700°C was estimated according to GOST 10145–81 using a ZST 2/3 tester.

The structure was examined by optical and scanning electron microscopy with an Olympus GX51 (SIAMS-700 image analysis software application) and JSM-6490LV microscopes, respectively. Metallographic polished sections were prepared according to a standard technique. Quantitative analysis was performed using the Image Expert Pro3x software application.

3. RESULTS AND DISCUSSION

3.1. Manufacturability of the VIT5 Alloy

Figures 1 and 2 show the results of the pressing tests performed in the temperature range 800–1100°C. Analysis of these results suggests that the VIT5 alloy exhibits the highest manufacturability at 1000°C, near the boundary between the three-phase ($\beta/B2 + \alpha_2 + O$) region and the two-phase ($\beta/B2 + \alpha_2$) one; and at 1100°C, which corresponds to the two-phase ($\beta/B2 + \alpha_2$) region. When the yield strength is reached ($\sigma_{0.2\text{comp}}^{1000} = 150 \text{ MPa}$, $\sigma_{0.2\text{comp}}^{1200} = 65 \text{ MPa}$), the stress continues to grow smoothly until the deformation degree is 50%. The compression curve changes at temperatures of 800–900°C. After the plastic flow zone ($\sigma_{0.2\text{comp}}^{800} = 980 \text{ MPa}$, $\sigma_{0.2\text{comp}}^{850} = 810 \text{ MPa}$, $\sigma_{0.2\text{comp}}^{900} = 555 \text{ MPa}$) is reached, first, the stress decreases significantly with increasing strain level; however, the stress again increases at $\epsilon = 40\text{--}50\%$. This deformation behavior of the alloy can be explained by structural transformations that occur at given temperatures.

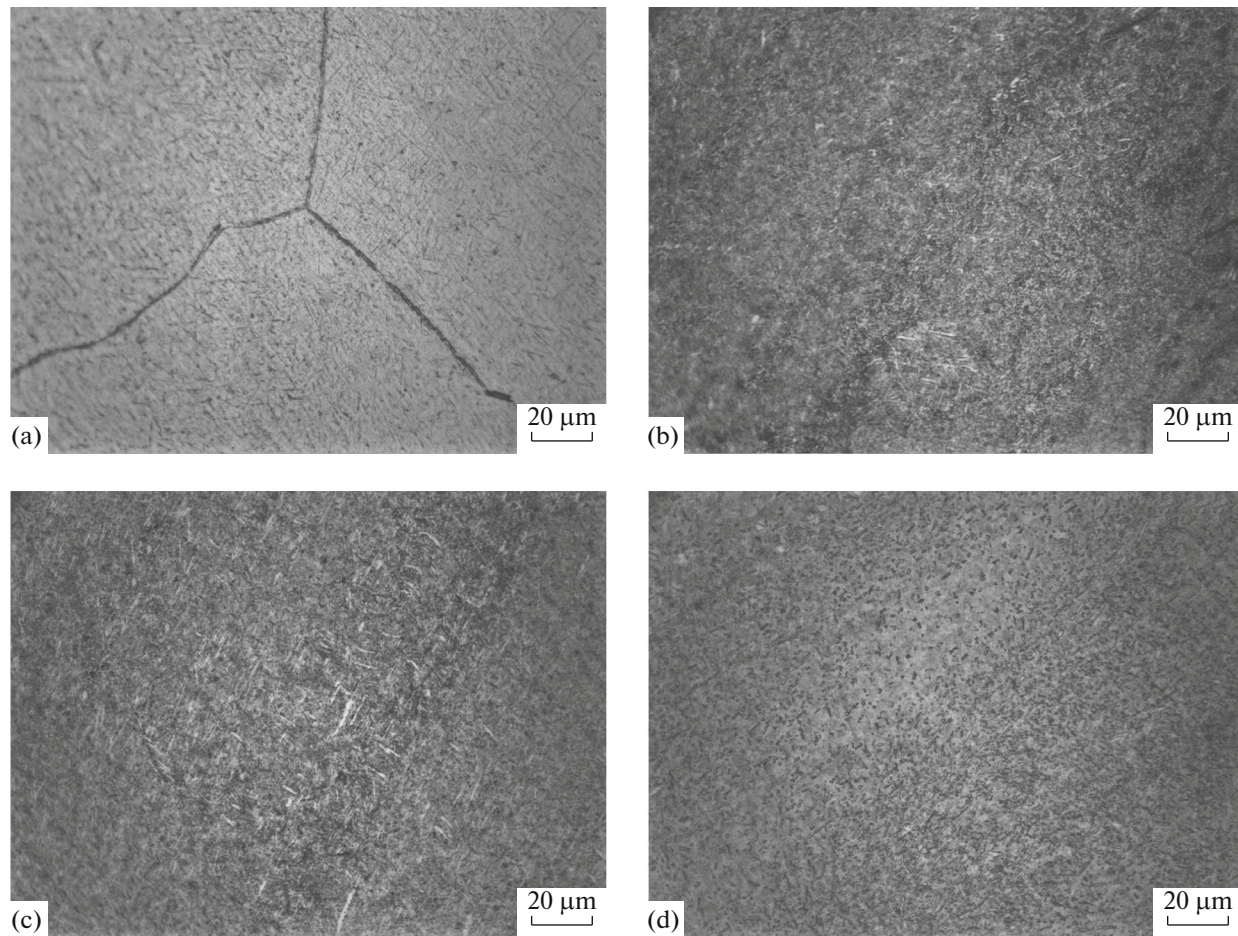


Fig. 3. Microstructure (optical microscopy) of the gadolinium-alloyed VIT5 ortho alloy (a) in the initial state and after compression at (b) 850, (c) 900, and (d) 1000°C.

The morphology and the volume fraction of O-phase precipitates depend on the deformation temperature (Fig. 3). The alloy structure after compression at 850 and 900°C consists of O-phase lamellae in the β /B2 matrix (see Figs. 3b, 3c). Lamellae become larger after the temperature increases by 50°C. After testing at 1000°C, there are two morphologies of O phase in the β /B2 matrix: globular and fine lamellar. The globular morphology results from the partial dissolution of the O-phase lamellae, existing in the cast material (see Fig. 3a), and their spheroidization during heating and holding at a test temperature. Lamellar-shaped O-phase precipitates form during the slow cooling of a sample together with the furnace. The offset yield strength decreases when the temperature increases from 850 to 1000°C (see Fig. 2) due to the dissolution of O-phase lamellae in the β /B2 matrix and the reduction in the volume fraction of the O phase.

Thus, the VIT5 intermetallic titanium alloy at first stages should be deformed at 1000°C and higher, since the material at these temperatures is the most technologically advanced and requires minimal strain loads.

This ensures that a cast structure can be developed by multiple forgings, defect-free deformed workpieces can be produced, and the load on the die tooling can be reduced.

3.2. Structure and Properties of the VIT5 Alloy after Rolling and Heat Treatment

A bimodal structure (Figs. 4a, 4c, 4e) forms in the plate treated according to regime 1. There are 2–6- μm particles of the globular O phase, fine (to 5 μm) and ultrafine (to 0.5 μm) O-phase lamellae in the matrix of the primary β /B2 phase. A bimodal structure (Figs. 4b, 4d, 4e) also forms in a rolled plate treated in regime 2; however, the size of globular O-phase particles decreases to 0.5–3.5 μm and the volume fraction of the particles decreases almost six times. The fine O-phase lamellae, which precipitate in the primary β /B2-phase matrix, increase in size (their length become 1–10 μm). Fine α 2-phase particles to 0.8 μm in size, which are clearly seen in reflected electrons, are observed along the boundaries of primary β /B2 grains (Fig. 5). In both cases, the structure

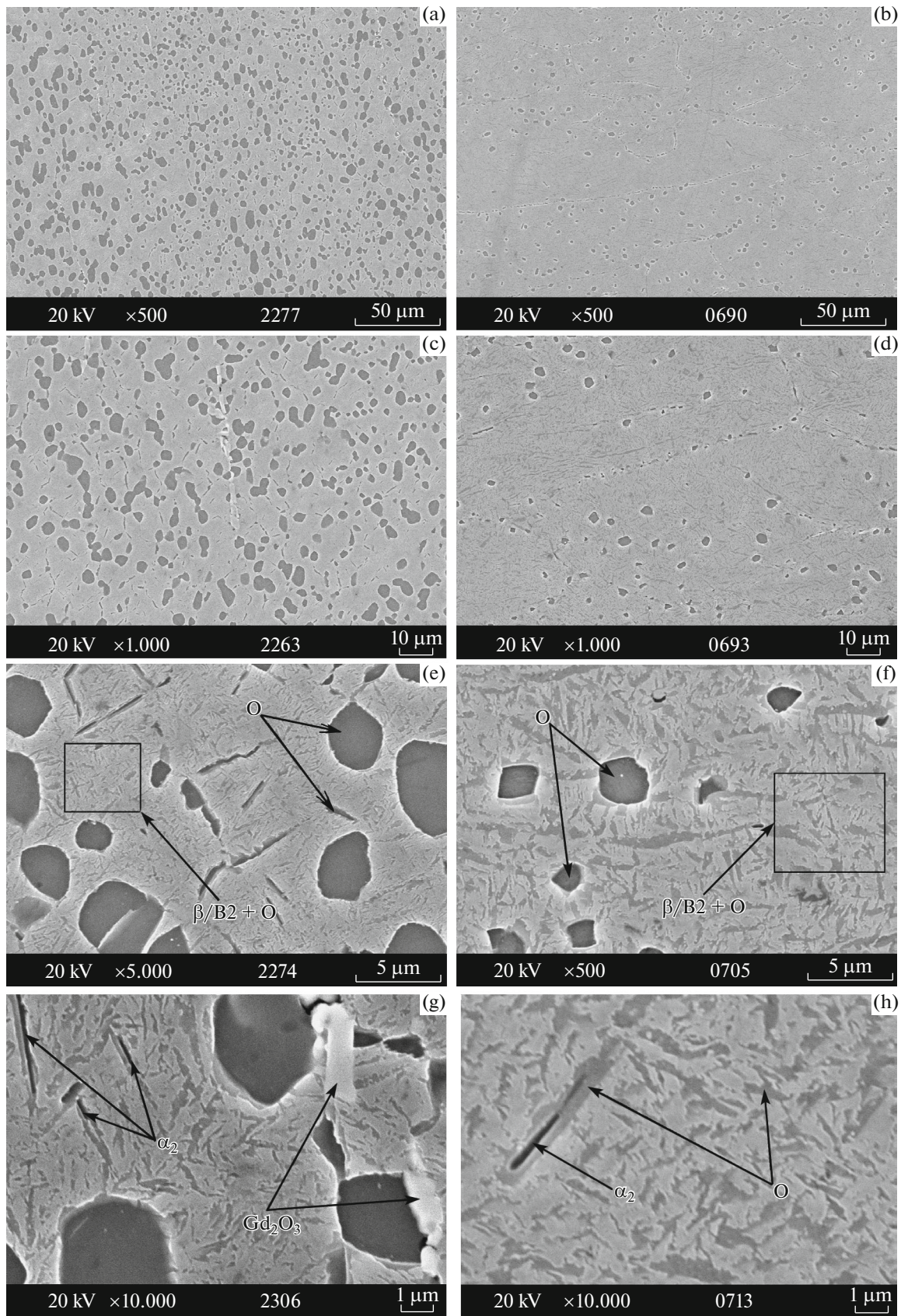


Fig. 4. Microstructure (SEM) of the rolled plates made of gadolinium-alloyed VIT5 ortho alloy after heat treatment: (a), (c), (e), (g) deformation regime 1 and (b), (d), (f), (h) deformation regime 2.

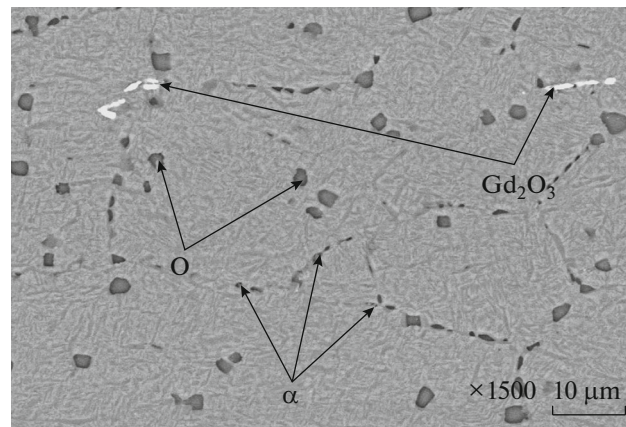


Fig. 5. Microstructure (SEM, backscattered electron regime) of the rolled gadolinium-alloyed VIT5 alloy plate after deformation according to regime 2.

exhibits the chains of Gd_2O_3 gadolinium oxides (see Figs. 4c, 4g, 5).

Mechanical tests were carried out to estimate the influence of the rolled plate microstructure formed in various deformation regimes on the level of performance properties. The investigation of mechanical properties at room and higher temperatures showed that the plates manufactured in regime 2 and having a lower volume fraction of the globular O phase at a comparable strength level at 20°C have higher plasticity and higher heat resistance characteristics than that treated in regime 1: short-term strength at 700°C is higher by 180 MPa, long-term strength at 700°C after 100-h testing is 1.5 times higher, and the relative elongation at room temperature is 1.5 times higher than those of the plates after regime 1 (Fig. 6).

Quantitative metallographic analysis (Table 1) was carried out to determine the volume fraction and the size of the globular O phase in the microstructure of the plates manufactured in regime 2, which possess the highest level of mechanical properties. The volume fraction of the globular O phase has been found to be about 3%. The globules are located both in a primary $\beta/B2$ grain and along its boundaries (see Fig. 5). The Gd_2O_3 particles are mainly located along the boundaries of the primary $\beta/B2$ grains and elongated in the rolling direction (Fig. 7). Coarse particles (to 16 μm in length) are arranged in a chain manner and represent a cluster of individual fine equally oriented particles (see Figs. 5, 7).

The volume fraction of Gd_2O_3 gadolinium oxides is 0.2% (see Table 1).

Table 1. Characteristics of the structural and phase constituents of the VIT5 alloy plates prepared according to regime 2

Parameter	O-phase globules	α_2 -phase particles	Gd_2O_3 particles
Volume fraction, %	2.94	1.51	0.20
Diameter of a circle with the equivalent area	1.54	1.31	1.75
Length, μm	2.07	1.41	3.32
Width, μm	1.37	1.08	1.10
Elongation	1.56	1.32	3.24
Maximum length, μm	5.55	7.71	16.21
Maximum width, μm	4.58	4.57	5.25
Shape parameter (P/S)*	5.35	4.29	5.40

* P is the perimeter of a particle and S is its area.

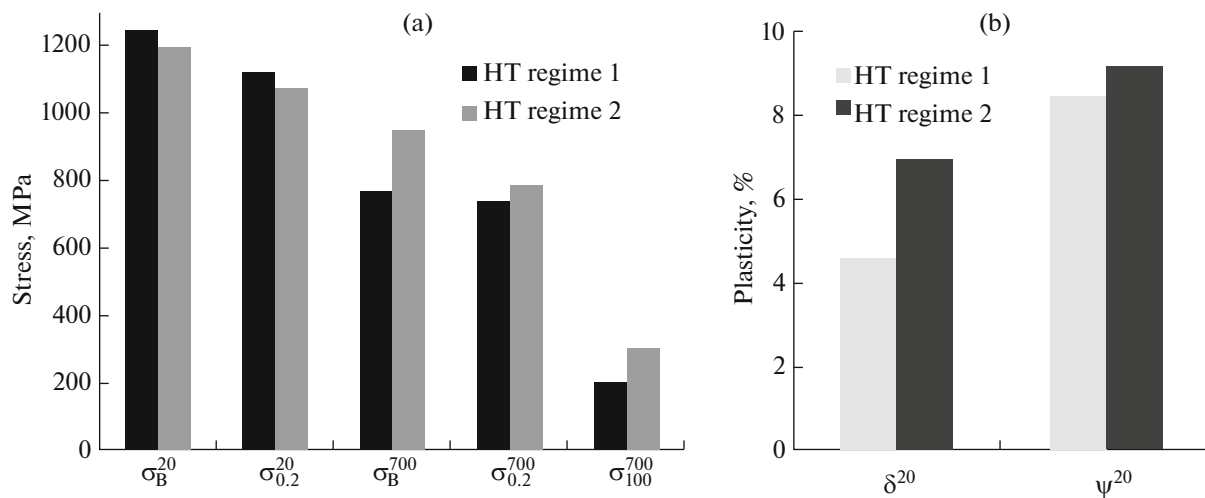


Fig. 6. (a) Strength and (b) plastic properties of the rolled gadolinium-alloyed VIT5 alloy plates after deformation in regimes 1 and 2 and subsequent heat treatment.

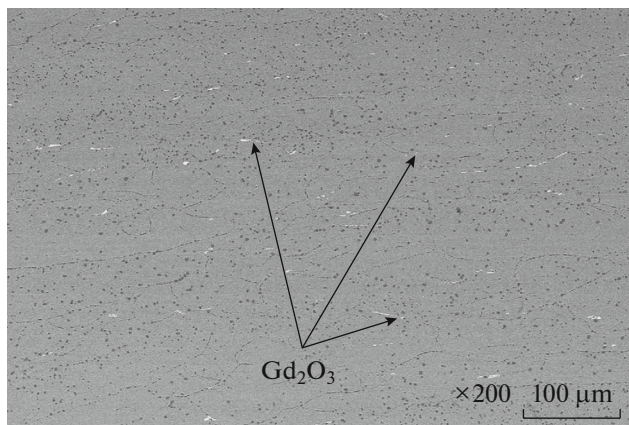


Fig. 7. Gd_2O_3 particle distribution (SEM, backscattered electron mode) of the rolled gadolinium-alloyed VIT5 alloy plate after deformation according to regime 2.

4. CONCLUSIONS

(1) The intermetallic VIT5 titanium ortho alloy with gadolinium microadditives shows the highest manufacturability at temperatures above 1100°C.

(2) The yield strength decreases when the temperature increases from 800 to 1000°C due to the dissolution of O-phase lamellae in the $\beta/B2$ matrix and the reduction in the volume fraction of the O phase.

(3) The formation of a bimodal structure with the globular O phase in the specified amount of 3 vol % and fine lamellar O-phase particles from 1 to 10 μm in size, which precipitate in the matrix of the primary $\beta/B2$ phase, increases the plastic properties and the heat resistance of the gadolinium-alloyed intermetallic titanium ortho alloy: $\delta^{20} = 7.0\%$, $\sigma_u^{700} = 950$ MPa, and $\sigma_{100}^{700} = 300$ MPa.

ACKNOWLEDGMENTS

The research was carried out using the certified and accredited equipment at the Test Center of All-Russia Institute of Aviation Materials VIAM.

The results were processed at the Competence Center for Development and Production of Titanium Intermetallic Alloys for Aircraft Engines and Terrestrial Power Plants (VIAM).

FUNDING

This work was carried out within the framework of complex scientific direction 7.1 Titanium-Based Intermetallic Alloys and Strategic Trends in the Development of Materials and Technologies of Their Processing for the Period until 2030 [24].

REFERENCES

1. H. Clemens and S. Mayer, "Intermetallic γ -titanium aluminide-based alloys from a metallographic point of view—A continuation," *Pract. Metallogr.* **48** (2) 64–99 (2011).
2. N. A. Nochovnaya, O. A. Bazyleva, D. E. Kablov, and P. V. Panin, *Titanium-Based and Nickel-Based Intermetallic Alloys*, Ed. by E. N. Kablov, (VIAM, Moscow, 2018).
3. E. V. Rodin, Yu. G. Bykov, and K. A. Kyaramyan, "Application of new materials in the design of HPC of an advanced engine," in *Proceedings of International Conference on Promising Trends in the Development of Aviation Engine Industry* (Skifiya, St. Petersburg, 2016), pp. 301–308.
4. E. N. Kablov, "New generation materials are the foundation for innovations, technological leadership, and national security in Russia," *Intellect Technol.* **14** (2), 16–21 (2016).

5. V. V. Antipov, "Outlook of aluminum, magnesium, and titanium alloys in the aerospace equipment," *Aviats. Mater. Technol.*, No. S, 264–271 (2017). <https://doi.org/10.18577/2071-9140-2017-0-S-186-194>
6. V. G. Antashev, N. A. Nochovnaya, T. V. Pavlova, and V. I. Ivanov, "High-temperature titanium alloys," in *All Materials. Encyclopedic Reference Book* (2007), No. 3, pp. 7–8.
7. *Titanium and Titanium Alloys. Fundamentals and Applications*, Ed. by C. Leyens and M. Peters (Wiley-VCH, Weinheim, 2003).
8. W. Chen, J. W. Li, L. Xu, and B. Lu "Development of Ti₂AlNb alloys: Opportunities and challenges," *Adv. Mater. Processes*. **172** (5), 23–27 (2014).
9. E. N. Kablov, O. G. Ospennikova, and A. V. Vershkov, "Rare metals and rare earth elements—materials of modern and high technologies of the future," *Trudy VIAM*, No. 2, St. 01 (2013). <http://www.viam-works.ru>. Cited January 16, 2019.
10. A. I. Khorev, N. A. Nochovnaya, and A. L. Yakovlev, "Microalloying with rare-earth metals of titanium alloys," *Aviats. Mater. Technol.*, No. S, 206–212 (2012).
11. Y.-Y. Chen, B.-H. Li, and F.-T. Kong, "Effects of minor yttrium addition on hot deformability of lamellar Ti–45Al–5Nb alloy," *Trans. Nonferrous Met. Soc. China*. **17** (1), 58–63 (2007).
12. Y.-Y. Chen, F.-T. Kong, J. Han, Z. Chen, and J. Tian, "Influence of yttrium on microstructure, mechanical properties and deformability of Ti–43Al–9V alloy," *Intermetallics* **13** (3, 4), 263–266 (2005).
13. J. Hieda, M. Niinomi, M. Nakai, and K. Cho, "Mechanical properties of biomedical β-type titanium alloy with rare-earth metal oxide particles formed by rare-earth metal addition," in *Proceedings of 143rd Annual Meeting and Exhibition TMS 2014* (Wiley, 2014), pp. 129–135.
14. C. M. Liu, K. Xia, and W. Li, "Effect of cerium on the microstructure and grain sizes of cast TiAl alloys," *J. Mater. Sci.* **35**, 975–980 (2000).
15. J.-R. Dai, H.-M. Lu, Z.-J. Cai, and C. An, "Grain refining or Er added to Ti–22Al–25Nb alloy and morphology of erbium precipitates," *Rare Met.* **32** (1), 5–11 (2013).
16. A. I. Khorev, G. P. Mukhina, and I. P. Zhegina, "Influence of Rare-Earth Elements on the Properties of Titanium Alloys," in *Alloying and Heat Treatment of Titanium Alloys* (VIAM, Moscow, 1977), pp. 106–114.
17. E. B. Alekseev, N. A. Nochovnaya, A. V. Novak, and P. V. Panin, "Yttrium-alloyed deformed intermetallic titanium ortho alloy. Part 1. Investigation of ingot microstructure and building the rheological curves," *Trudy VIAM*, **66** (6), 12–21 (2018). <https://doi.org/10.18577/2307-6046-2018-0-6-12-21>
18. E. B. Alekseev, N. A. Nochovnaya, A. V. Novak, and P. V. Panin, "Yttrium-alloyed deformed intermetallic titanium ortho alloy. Part 2. The effect of heat treatment on the microstructure and mechanical properties of a rolled plate," *Trudy VIAM*, **72** (12), 37–45 (2018). <https://doi.org/10.18577/2307-6046-2018-0-12-37-45>
19. Y.-F. Si, Y.-Y. Chen, Z.-G. Liu, and F.-T. Kong, "Influence of yttrium on microstructure and properties of Ti–23Al–25Nb alloy after heat treatment," *Trans. Nonferrous Met. Soc. China*. **16**, 849–853 (2006).
20. Niu Hongzhi, Zhang Yusheng, Lu Jinwen, Zhang Wei, Zhang Pingxiang, "Ti₂AlNb alloy with low density and high plasticity," CN Patent 104372202, 2015.
21. N. A. Nochnovnaya, E. B. Alekseev, P. V. Panin, and A. V. Novak, "Investigation of the structure and mechanical properties of the deformed intermetallic VIT5 gadolinium-alloyed titanium alloy," *Titanium*, No. 2, 21–29 (2017).
22. E. N. Kablov, N. A. Nochovnaya, P. V. Panin, E. B. Alekseev, and A. V. Novak, "Study of the structure and properties of heat-resistant alloys based on titanium aluminides with gadolinium microadditives," *Inorg. Mater. Appl. Res.*, No. 3, 3–10 (2017).
23. E. B. Alekseev, N. A. Nochovnaya, S. V. Skvortsova, P. V. Panin, and O. Z. Umarova, "Analysis of technological parameters of deformation of experimental heat-resistant alloy based on Ti₂AlNb intermetallic compound," *Titan*, No. 2, 34–39 (2014).
24. E. N. Kablov, "Innovative developments of the FSUE VIAM SSC of RF for the realization of Strategic Directions in Developing Materials and Their Processing Technologies up to 2030," *Aviats. Mater. Technol.* **34** (1), 3–33 (2015). <https://doi.org/10.18577/2071-9140-2015-0-1-3-33>

Translated by T. Gapontseva